1 Glacier inventories reveal an acceleration of
2 Heard Island glacier loss over recent decades

3 **Levan G. Tielidze[1,2], Andrew N. Mackintosh[1,3], Weilin Yang[3]**

4 [1]Securing Antarctica's Environmental Future, School of Earth, Atmosphere and
5 Environment, Monash University, Clayton, VIC 3800, Australia

6 [2]School of Natural Sciences and Medicine, Ilia State University, Tbilisi 0162, Georgia

7 [3]School of Earth, Atmosphere and Environment, Faculty of Science, Monash University,
8 Clayton, VIC 3800, Australia

9 **Abstract**

10 Glacier inventories provide baseline data for understanding and evaluating past, current,
11 and future changes in glacier extent in response to climate changes. We present a multi-
12 year, manually mapped glacier inventory for sub-Antarctic Heard Island, a remote
13 glacier-covered volcano in the southern Indian Ocean. Glacier outlines are presented for
14 1947, 1988, and 2019, derived from large-scale topographical maps (1:50,000), cloud-
15 free medium-resolution SPOT, and high-resolution Pléiades satellite orthoimages. ASTER
16 and Pléiades digital surface elevation models for 2000 and 2019 were also used to
17 determine topographic parameters for individual glaciers. Heard Island glacier area
18 reduced from 289.4±6.1 km^2 in 1947 to 260.3±6.3 km^2 in 1988, further decreasing to
19 225.7±4.2 km^2 in 2019. The rate of annual glacier area loss between the two observation
20 periods (1947-1988 and 1988-2019) almost doubled from −0.25% yr^{-1} to −0.43% yr^{-1}.
21 Glaciers on the eastern slopes of Heard Island experienced much higher retreat rates
22 than glaciers elsewhere on the island. The maximum retreat observed between 1947 and
23 2019 was ~5.8 km for the east-facing Stephenson Glacier, where collapse of the terminus
24 led to the formation of a large lagoon during recent decades. Surface debris cover on
25 Heard Island glaciers increased from 7.0±6% (18.1 km^2) in 1988 to 12.8±5.5% (29.0 km^2)
26 in 2019. We also observed an upward shift (4.2 m yr^{-1}) in the maximum elevation of debris
27 cover from 285±20 m a.s.l. (above sea level) to 605±20 m a.s.l., during this time. Direct
28 climate observations from Heard Island are scarce, but reanalysis climate data show that
29 the decline in glaciers is associated with a rising temperature of 0.7°C over the last seven
30 decades. Many questions about the behaviour of Heard Island glaciers remain
31 unanswered. Our inventory dataset will be freely available in the GLIMS glacier database
32 to facilitate further analysis and modelling of Heard Island glaciers.

33

34 **Correspondence:** Levan G. Tielidze (tielidzelevan@gmail.com)

35

36 **Keywords:** Heard Island, glacier inventory, remote sensing, debris cover, glacier retreat.

1 Introduction

Glaciers are a key component of the climate system and serve as sensitive indicators of climate change (Hock et al., 2019). Over recent decades, global glaciers—excluding the Greenland and Antarctic ice sheets—have contributed approximately 27 ± 22 mm to the rise in global mean sea level from 1961 to 2016. This represents 25 to 30 percent of the total sea level rise during that period (Zemp et al., 2019). Glacier retreat also has a fundamental impact on global water supplies and mountain hazards (Hock et al., 2019) and glacier inventories are essential for assessing all these impacts (Haeberli and Hoelzle 1995). Inventories include digitized glacier outlines and their morphological features, such as area, slope, aspect, and elevation, mapped from satellite images and Digital Elevation Models (DEMs). They provide crucial data for estimating geodetic mass balance (Shean et al. 2020), determining glacier volume (Farinotti et al. 2019), measuring surface velocity (Dehecq et al. 2019), and testing glacier models (Radić et al., 2014; Eis et al., 2021).

Given the scarcity of landmasses and climate observations in the Southern Ocean region, glacier-covered sub-Antarctic islands provide a unique window into the impacts of past, present, and future climate changes (e.g. Deline et al., 2024). Heard Island is such an example but because of its harsh climate and remote location, its glaciers remain relatively poorly studied compared to other mid-latitude glaciers in the Southern Hemisphere. A new inventory from this region offers critical data on glacier behaviour, such as area and terminus changes, which are essential for understanding how these glaciers are responding to climate changes and other drivers. Given the limited field-based research opportunities on Heard Island, a new glacier inventory also allows us to analyse past glacier conditions, improving our understanding of processes and providing a baseline for predicting future changes in this sensitive region.

Heard Island is an UNESCO World Heritage site due to its outstanding physical and biological features which are being affected by significant on-going climatic changes. As one of the only sub-Antarctic islands mostly free of introduced species, its ecosystems are particularly at risk from the impact of glacier retreat (HIMI Management Plan, 2014). Glacier inventory work will help in designing effective conservation strategies and managing protected areas to ensure the preservation of the biodiversity they support (Pockley, 2001; HIMI Management Plan, 2014).

Since a complete inventory of Heard Island glaciers has not been published for several decades (e.g. Budd, 2000; Allison and Thost, 2000; Thost and Truffer, 2008), this study aims to create a new inventory using remotely sensed glacier parameters. We use our analysis to assess how various climatic, morphological and topographic factors influence glacier recession on Heard Island, providing preliminary answers to the question of how and why Heard Island glaciers are changing.

2 Study area

2.1 Physical characteristics

Heard Island is the largest member of the Territory of Heard Island and McDonald Islands located at 53°05'S latitude and 73°31'E longitude at the southern edge of Indian Ocean, almost midway between western Australia and South Africa. Antarctica is the nearest continent, located ~1500 km to the south, while the relatively large Kerguelen Islands are ~450 kilometers to the northwest. Heard Island is approximately 40 km long from northwest to southeast, and only 20 kilometers wide from northeast to southwest (Figure 1).
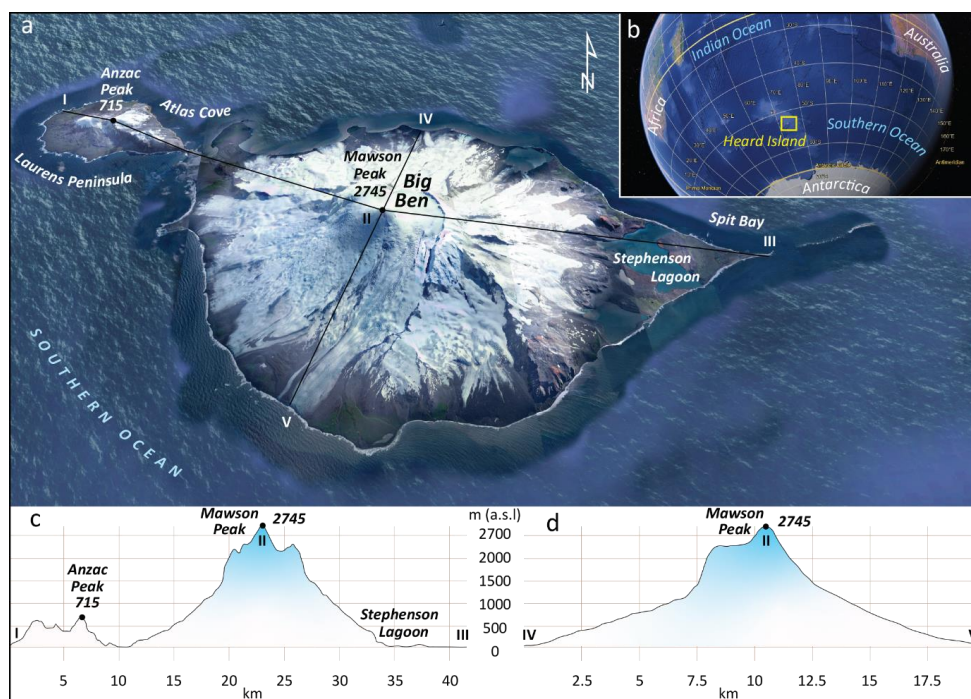
Figure 1. True colour aerial image of the Heard Island (© Google Earth). b - location of the Heard Island in the Southern Hemisphere (© Google Earth). c - Longitudinal and d - transverse profiles (cross sections) of Heard Island.

Heard Island, along with the McDonald Islands and Kerguelen Island, forms part of the submarine Kerguelen Plateau, a significant geological feature in the southern Indian Ocean. Heard Island's geological structure is characterized by its two volcanic cones — Big Ben and Laurens Peninsula — each with distinct elevations and volcanic rocks and landforms. Big Ben, with a diameter of ~20 km and reaching an elevation of 2,745 m asl at Mawson Peak, is the larger volcanic cone. The highest point of the Laurens Peninsula

97   is Anzac Peak (715 m asl). Over 80% of the Heard Island is ice-covered with glaciers
98   (Thost and Truffer, 2008) flowing from the caldera of Big Ben and the summit plateau of
99   Laurens Peninsula. Big Ben was most recently reported active in November 2020 (Fox et
100   al., 2021).

101   The climate of the Heard and McDonald Islands region is significantly shaped by its mid-
102   latitude position in the Southern Ocean, south of the Antarctic Polar Front, where
103   subantarctic and colder Antarctic Ocean waters converge. This location is affected by
104   the region's westerly winds, which are linked to the west-to-east progression of deep low-
105   pressure systems in the mid to high southern latitudes (Allison and Keage, 1986). Heard
106   Island's weather is characterized by small variations in both seasonal and daily
107   temperatures, with persistent cloud cover, frequent precipitation, and strong winds.
108   Snowfall occurs year-round. Based on various observations from the second half of the
109   20th century (Kiernan and McConnell, 2002; HIMI official website, last access: August
110   2024), average monthly temperatures at Atlas Cove range from 0.0 to 4.2°C. In summer,
111   daily temperatures typically vary between 3.7 and 5.2°C, while in winter, they range from
112   −0.8 to 0.3°C. The winds are predominantly westerly and strong, with monthly average
113   speeds at Atlas Cove varying between ~26 and 33.5 km/h. Gusts can exceed 180 km/h.
114   Heard Island experiences annual precipitation at sea level ranging from 1,300 to 1,900
115   mm, with rain or snow occurring on roughly three out of every four days. However,
116   meteorological records for the island are scarce and incomplete and long-term local
117   observations including information about local gradients and trends are absent.

118

119   **2.2 Previous studies**

120   Heard Island became widely known after 1853 when Captain Heard visited the site,
121   although it was first seen by Captain Peter Kemp in 1833 (Mawson, 1935). Two years after
122   Captain Heard's expedition, Darwin Rogers was the first to land on Heard Island in 1855
123   (Lambeth, 1951). Following this, sealers occupied the island from the mid to late 19th
124   Century, decimating the seal population. Later, various scientific expeditions visited
125   Heard Island and stayed only several days, mainly at Atlas Cove (e.g. Drygalski, 1908;
126   Aubert de la Rue, 1929; Mawson, 1932).

127   The largest scientific campaign began in 1947, when the Australian National Antarctic
128   Research Expedition established a base camp at Atlas Cove. This campaign continued
129   until 1955, and James Lambeth first carried out physical measurements of Heard Island
130   glaciers at this time (Lambeth, 1951). According to his notes the snow line of the Heard
131   Island glaciers was at about 305 m a.s.l. in Austral summer of 1947-1948. There was
132   minor difference in the snowline elevations between north- and south-facing glaciers.
133   Thickness of the Baudissin and Vahsel glaciers at the frontal area was between 35-40 m
134   in August 1948. Ice velocity measurement at an elevation of 90 m a.s.l. of Baudissin
135   Glacier tongue between 11 September and 8 December indicated an average ice flow

136 rate of approximately 440 m a^{-1}, while the ablation at an elevation of about 40 m a.s.l. was
137 ~−0.35 m during this ~33-month period.

138 Short scientific visits to the island were also made in 1963, 1965 and 1969 mainly for
139 seasonal observation of the north-facing glacier front variations (Budd, 1964; 1970; Budd
140 and Stephenson, 1970). More detailed studies of Vahsel Glacier, including mass balance
141 measurements started later in 1971 (Allison 1980). Ablation at 200 m a.s.l. was estimated
142 at 3-4 metres water equivalent annually. A surface velocity profile across the glacier at
143 the same elevation showed annual movement of 200-280 m near the centre. Average
144 thickness of Vahsel Glacier (determined gravimetrically) below the equilibrium line, was
145 between 60-80 m near the centreline.

146 Studies of south and southeast facing glaciers starter later in 1990s. The retreat and
147 proglacial lake expansion at Stephenson Glacier was studied by Kiernan and McConnell
148 (2002), who showed that the glacier retreated at a mean rate of -18 ma^{-1} from 1947 to
149 1987 before accelerating dramatically to -100 m a^{-1} between 1987 and 2000. Further
150 glaciological and meteorological study of Brown Glacier on the eastern slope of Heard
151 Island was conducted by Thost and Truffer (2008) based on old topographical maps
152 (1947) and ground-based observations (2004). They concluded that Brown Glacier area
153 decreased by ~29% during the investigated period, while on average the surface lowered
154 by −0.50 m a^{-1}. This mass loss was consistent with interpolated summer (January-March)
155 temperatures in the area that indicated a +0.9 °C warming over the investigated period
156 (1947-2004). They also observed that the Brown Glacier terminus retreated by 63 m
157 between 2000 and 2003.

158 The GLIMS book (Kargel et al., 2014) identifies 29 glaciers on Heard Island with a total
159 area of 257 km^2 in 1988 (Cogley et al., 2014), while the Randolph Glacier Inventory (RGI6)
160 database identifies 31 glaciers with a total area of 254.4 km^2. Some glaciers in these
161 datasets have incorrect terminus positions, specifically the eastern-facing glaciers, and
162 nearly all glaciers are also characterized with inaccurate ice margins (due to
163 misidentification of ice divides). This issue persists in the RGI7 database (Maussion et al.,
164 2023).

165

166 **3 Data sources**

167 Conducting large-scale field-based glacier research on Heard Island is extremely
168 challenging due to topographic, logistical, financial, and safety obstacles (e.g. Allison
169 and Thost, 2000). Consequently, old topographical maps and remotely sensed images
170 from historical and current Earth observation platforms provide the most viable method
171 for tracking changes in glacier parameters (e.g. Tielidze, 2016; Freudiger et al., 2018;
172 Weber et al., 2020).

173

3.1 Old maps

The first aerial photographs of Heard Island glaciers were captured in 1947 using a hand-held 6" x 6" Fairchild F24 camera aboard an RAAF Walrus amphibious aircraft. These photos provided limited oblique coverage of the east and north coasts. However, a ground triangulation survey conducted in 1948, which focused on Laurens Peninsula and the north and east coasts, allowed for more accurate mapping of terrain features, including glacier fronts (Allison 1980). A large scale (1:50,000) topographical map of Heard Island (1964) shows glacier boundaries from 1947-1948 based on these early photographs and surveys (Division of National Mapping, 1964). Therefore, the glacier extent on Heard Island in 1947-1948 can be directly referenced from this topographical map, which reflects the original positions of the glaciers as depicted in the aerial images (Figure 2; Table 1).
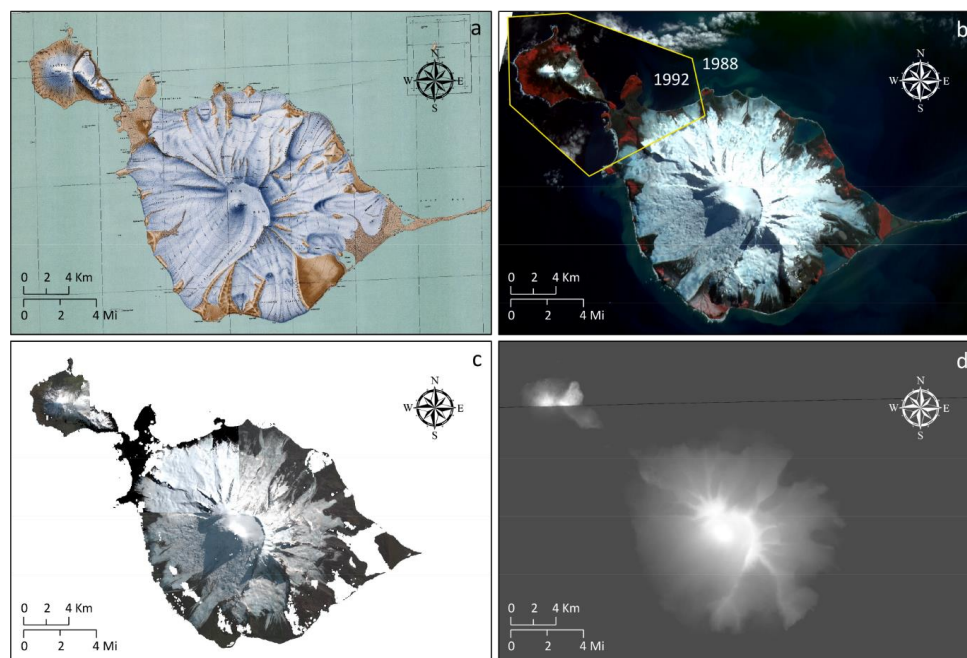
Figure2. Data sources used in this study for glacier mapping. a – Topographical map from 1964 compiled based on aerial imagery from 1947. b – SPOT images from 1988 and 1992. c – Pléiades images from 2019; d – ASTER DEM from 2000.

3.2 Satellite images

Although Landsat satellite products have been available since the 1980s, the frequent cloud cover around Heard Island has obscured the glaciers partially or completely, making it difficult to accurately delineate glacier boundaries. We therefore use medium-

196   resolution (10 and 20 m) cloud-free SPOT 1 images from 1988 and 1992 available from
197   the French Space Agency (CNES)'s Spot World Heritage Programme
198   (https://regards.cnes.fr/html/swh/Home-swh3.html, accessed August 2024). The 1988
199   image was used as the baseline database, and the 1992 image was used as a supplement
200   because the Laurens Peninsula and northern parts of the Heard Island glaciers were
201   partly covered by clouds in 1988 image.

202   A 2-metre resolution, georeferenced, cloud-free Pléiades ortho mosaic and 0.5-metre
203   resolution panchromatic bands from 2019 austral summer were used to delineate the
204   most recent glacier boundaries in our data set. These images were not available for the
205   northwest part of the Laurens Peninsula. To fill this gap, we used similar Pléiades product
206   acquired in April 2018, but the images from 2019 were used as a main dataset for the
207   island. Pléiades images were received from the Laboratory of Space Geophysical and
208   Oceanographic Studies (LEGOS) via the Pléiades Glacier Observatory (Berthier et al.,
209   2024).

210   High-resolution QuickBird images (2014-2024), combined with SRTM3 topography data
211   (Raup et al., 2014), were also used in Google Earth Pro software to enhance the 3D
212   visualization and identification of ice divides as well as to validate the glacier outlines
213   mapped from the satellite images.

214   For the annual measurements of Stephenson and Brown glacier termini, a 30 m
215   resolution Landsat 7 Enhanced Thematic Mapper Plus (ETM+) and 10 m resolution
216   Sentinel 2 images were used, as they only had cloud-free windows for these two glaciers.
217   Both Landsat and Sentinel products are from the Earth observation (EO) Browser
218   (https://apps.sentinel-hub.com/eo-browser/ accessed August 2024).

219

3.3 Digital elevation/surface models

221   Topographic parameters of glaciers such as aspect, slope, and elevation from 1947 and
222   1988 were obtained from the Advanced Spaceborne Thermal Emission and Reflection
223   Radiometer Global Digital Elevation Model (ASTER GDEM V2, March 1, 2000), available
224   through the EarthExplorer (http://earthexplorer.usgs.gov/, accessed May 2024), U.S.
225   Geological Survey (USGS), with a horizontal resolution of 20 meters (Tachikawa et al.,
226   2011). The ASTER GDEM is widely recognized and used in glaciological research globally
227   across different spatial scales (e.g. Bhambri et al. 2011; Stokes et al., 2013; Tielidze et
228   al., 2020). The same topographic characteristics for the glaciers from 2019 were
229   extracted from the high-resolution (2 m) Pléiades Digital Surface Models (DSM) 2018-
230   2019 available from the Laboratory of Space Geophysical and Oceanographic Studies
231   (LEGOS) via the Pléiades Glacier Observatory (Berthier et al., 2024).

232

233 **Table 1**. Topographic maps, satellite images and digital elevation/surface models used in
234 this study.

Product	ID	Date	Resolution/Scale
Map			
Topographical map	G9182.H4	1964 (1947)	1:50 000
Satellite image			
SPOT 1	1 245-457 88-01-09 04:47:36 1 X	09/01/1988	10 m
SPOT 1	2 245-458 92-03-24 05:00:31 1 X	24/03/1992	20 m
Landsat 7 ETM+	LE07_L2SR_135097_20010131_20200917_02_T1	31/01/2001	30 m
Landsat 7 ETM+	LE07_L2SR_135097_20030105_20200916_02_T1	05/01/2003	30 m
Landsat 7 ETM+	LE07_L2SR_135097_20040312_20200915_02_T2	12/03/2004	30 m
Landsat 7 ETM+	LE07_L2SR_135097_20050126_20200914_02_T1	26/01/2005	30 m
Landsat 7 ETM+	LE07_L2SR_135097_20080204_20200913_02_T1	04/02/2008	30 m
Landsat 7 ETM+	LE07_L2SR_135097_20090206_20200912_02_T1	06/02/2009	30 m
Landsat 7 ETM+	LE07_L2SR_135097_20100209_20200911_02_T1	09/02/2010	30 m
Sentinel 2 L2A	42/F/YF/2017/4/16/0/	16/04/2017	10 m
Pléiades	0444140_Heard_ANT_1B	22/04/2018	0.5-2 m
Pléiades	0451575_Heard_ANT_1B	07/04/2019	0.5-2 m
Pléiades	0452069_Heard_ANT_1B	07/04/2019	0.5-2 m
Pléiades	0448386_Heard_ANT_1A	21/11/2019	0.5-2 m
Digital elevation/surface model			
ASTER	ASTGTMV003_S53E073	01/03/2000	20 m
ASTER	ASTGTMV003_S54E073	01/03/2000	20 m
Pléiades	0444140_Heard_ANT_1B	22/04/2018	2 m
Pléiades	0451575_Heard_ANT_1B	07/04/2019	2 m
Pléiades	0452069_Heard_ANT_1B	07/04/2019	2 m
Pléiades	0448386_Heard_ANT_1A	21/11/2019	2 m

235

236 **4 Methods**

237 *4.1 Glacier mapping*

238 Despite some advantages of the automated mapping method of clean ice (e.g. Paul et
239 al., 2013), manual mapping of glaciers is more suitable for many mountain regions
240 around the world (e.g. Stokes et al., 2013; Nagai et al., 2016; Tielidze and Wheate, 2018;
241 Korneva et al., 2024). In this study, glacier boundaries were, therefore, delineated
242 manually. This was also mainly due to the i) unavailability of cloud-free satellite
243 channels/bands for different years for the entire study area, which limited us to use
244 different band ratio segmentation methods for automated mapping; ii) significant
245 amount of debris-cover, which can cause uncertainty during automatic mapping; and iii)
246 a relatively small study area, which was less time expensive than it would have been for
247 an entire mountain range.

248

4.2 Terminus measurement

Accurately quantifying changes in glacier termini is essential for effective monitoring of glacier changes over various timescales, from days to centuries. Methods for this technique each offer advantages and limitations (Lea et al., 2014). In this study, we only measured two glacier (Stephenson and Brown) lengths based on the Global Land Ice Measurements from Space (GLIMS) guidelines (www.glims.com) and by following Purdie et al. (2014). The flow direction of the glacier was manually determined to be perpendicular to altitude contours. We assessed terminus changes by comparing glacier outlines from different dates along the ice front, oriented perpendicular to the flow. Elevation changes at the glacier fronts were also measured at the intersection points.

4.3 Accuracy and uncertainly assessment

When using glacier outlines to assess changes, it's crucial to understand their accuracy. Assessing accuracy can be difficult because high-resolution reference data are often scarce. Additionally, any manual corrections made to the raw outlines (e.g. such as debris cover) may reflect the bias of the analyst rather than the effectiveness of the algorithm used (Paul et al., 2013). It is therefore essential to establish an uncertainty even after achieving high-accuracy mapping. Uncertainty often arises from the resolution of the satellite image, and from the contrast between the glacier and the surrounding terrain (Burgess and Sharp, 2004; DeBeer and Sharp, 2007). To estimate the statistical uncertainty for each glacier, we used the buffer method as in Granshaw and Fountain (2006) and Bolch et al. (2010). This approach provides a minimum and maximum area values, which we utilized to calculate the relative area difference. For the 1:50,000 scale topographic map, or glacier outlines from 1947, a 30 m buffer size proposed by Tielidze (2016) was used, yielding a total potential error of ±2.1%. A 20 m buffer was used for 1988 glacier outlines giving a total error of ±2.4%. The chosen buffer is based on a previous multiple digitizing experiment from similar resolution satellite images worldwide (Paul et al., 2013; Tielidze and Wheate, 2018), demonstrating that the variability in positioning typically falls within one pixel, or approximately ±10-30 meters, depending on the image resolution. Despite the high resolution of the Pléiades images, we choose a 10 m buffer size for glacier contours from 2019 estimating a total uncertainty of ±1.9%. This decision is primarily due to an extensive debris cover, which frequently complicates the mapping of glaciers.

A larger buffer should be applied to the debris-covered parts of glaciers, as ouline uncertainties are higher than for bare ice (e.g., Tielidze et al., 2020). In our case, the buffer size was set to 30 meters, resulting in a total potential error of ±6.0% for 1988 and ±5.5% for 2019 glaciers. We have not estimated the surface debris cover for the glaciers from 1947.

287 For uncertainties in length changes, we used the source image resolution as proposed by
288 Hall et al. (2003).

289

290 **5 Results**

291 **5.1 Glacier area changes in 1947-1988-2019**

292 A total of 29 glaciers, with an average size of 9.9 km^2, were mapped in the study area in
293 1947 (Figure 3). During the 41-year observation period from 1947-1988, the glaciers
294 shrank by 29.1±0.7 km^2 (10.1%) from 289.4±6.1 km^2 in 1947 to 260.3±6.3 km^2 in 1988,
295 showing a mean annual glacier area loss of −0.25% yr^{-1}. 30 glaciers were identified in
296 1988 with an average size of 8.7 km^2. Between 1988 and 2019, a considerable decrease
297 in glacier area of 34.6 km^2 (13.3%) to 225.7±4.2 km^2 occurred, almost doubling the rate
298 of annual glacier area loss to −0.43% yr^{-1}. The average glacier size also decreased to 6.4
299 km^2 during this period.

300

301

302

10
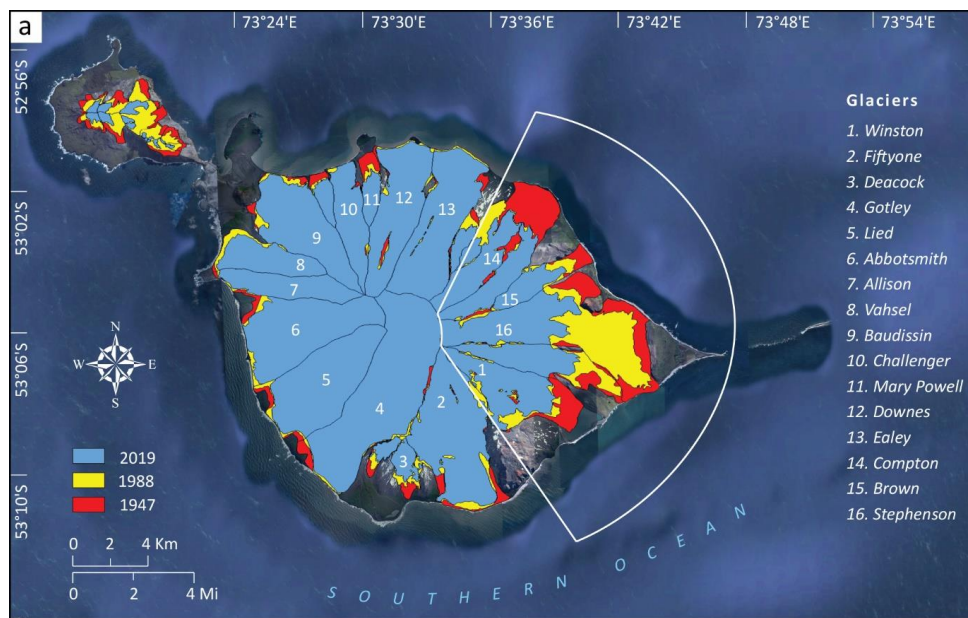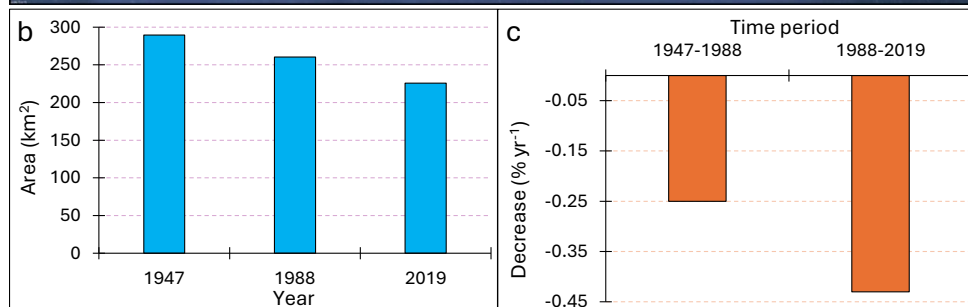
303 **Figure 3**. a - Heard Island glacier outlines in 1947, 1988, and 2019. The white frame
304 highlights east-facing glaciers where the highest decrease rates occurred. b - Heard
305 Island glacier areas in 1947, 1988, and 2019; c - Glacier area decrease rates for the Heard
306 Island for the two observed periods (1947-1988 and 1988-2019).

307

308 The pattern of observed glacier wastage is strongly influenced by topographic and
309 morphological parameters. The small and low elevation glaciers at Laurens Peninsula
310 experienced largest change in area from 10.5 km^2 to 2.2 km^2 between 1947-2019. This is
311 an area loss of 79±2.2% amounting to an annual decrease of −1.1% yr^{-1}.

312 We also observed upward shift of the minimum and mean elevation of all Heard Island
313 glaciers during the study period and downward shift of the maximum elevation from 1988
314 (Figure 4).

315
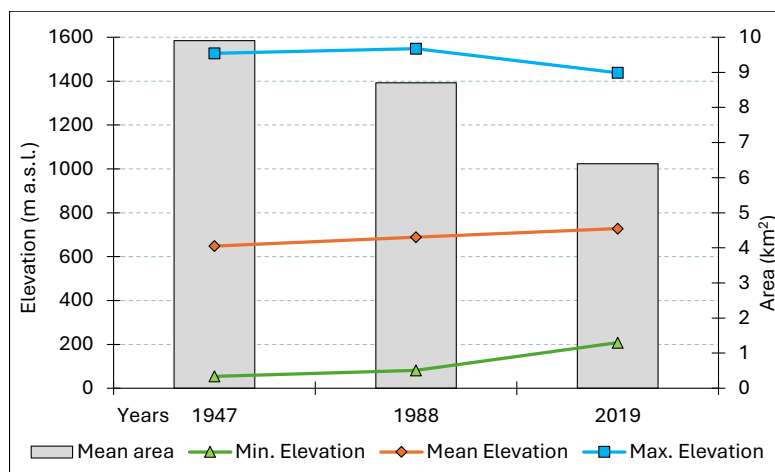
316

317 **Figure 4**. Changes in Heard Island glacier area and elevations between 1947-1988-2019.
318 Mean area, minimum (Min.), mean, and maximum (Max.) elevations are shown.

319

320 Gotley Glacier was largest on Heard Island in 2019, with an area of 32.3 ± 0.5 km^2,
321 followed by Fiftyone and Abbotsmith glaciers with areas of 21.8 ± 0.4 and 19.9 ± 0.3 km^2,
322 respectively.

323 The inventory shows that Heard Island glaciers are predominantly oriented towards the
324 northeast, while the largest glaciers are oriented southwest. Glaciers of west and
325 southwest orientation have the highest mean elevations (Figure 5a-c).

326 Eastern facing glaciers experienced the highest area loss over the study period (depicted
327 by the white outline in Figure 3a) from 85.1 ± 1.6 km^2 in 1947 to 66.5 ± 1.3 km^2 in 1988 and
328 46.3 ± 0.9 km^2 in 2019. This was a 22% or −0.53% yr^{-1} decrease between 1947-1988 which

329   is more than double than the change for all Heard Island glaciers over this period. Glacier
330   change during the more recent investigated period was dramatic and unprecedented for
331   the eastern facing glaciers on Heard Island - they declined by 30% or −1.0% yr⁻¹ between
332   1988-2019.

333

334

335

336
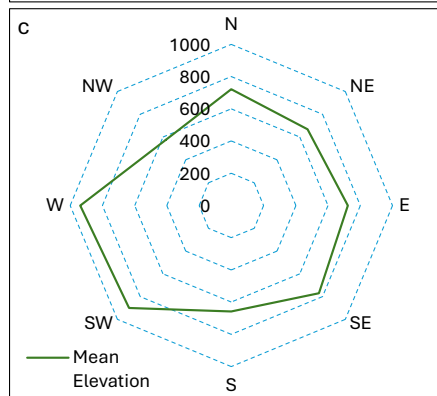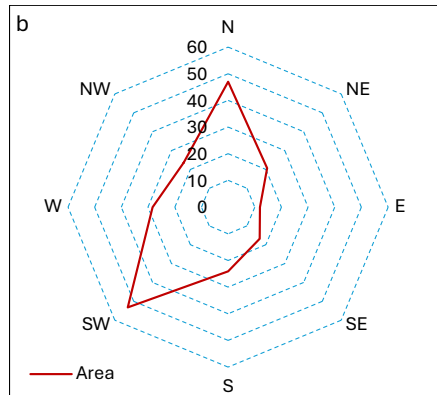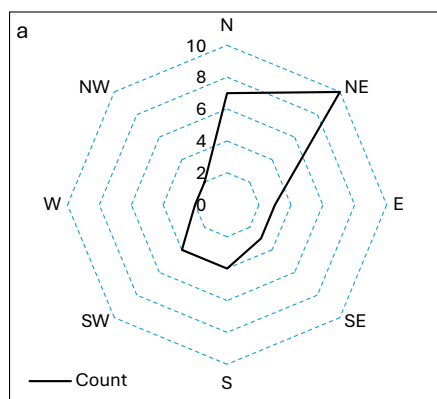
337   **Figure 5**. Distribution of Heard Island glacier aspects by (a) number, (b) area (km²) and (c)
338   mean elevation (a.s.l.) in 2019.

339

5.2 Glacier length changes

341 Brown and Stephenson glaciers showed significant terminus retreat, as evidenced by
342 glacier shrinkage during the study period. Average total terminus retreat of 1483±20 m
343 was observed for Brown Glacier between 1947–2019 with an annual mean retreat rate of
344 −20.6 m yr^{-1} (Figure 6a). The retreat rate of −25.7 m yr^{-1} was much higher during the
345 second investigated period (1988-2019).

346

347

348
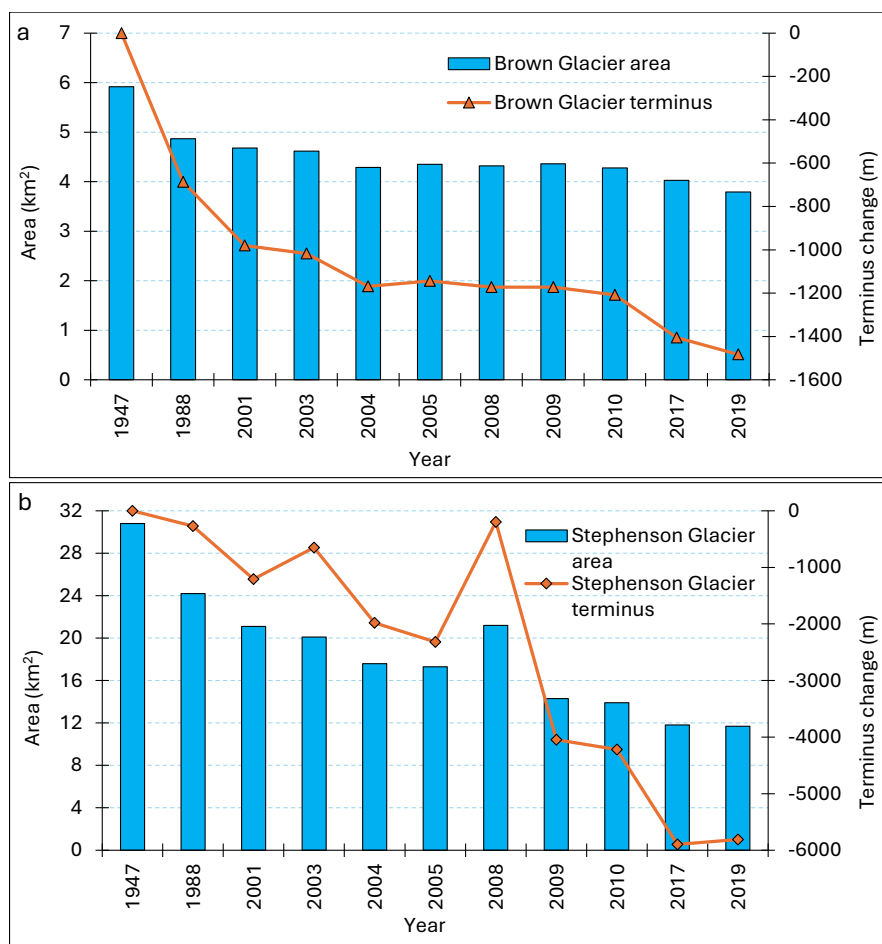
Figure 6. Cumulative terminus and area changes for Brown (a) and Stephenson (b)
350 glaciers between 1947 and 2019.

351

352 Stephenson Glacier retreated more than any other glacier on Heard Island during our
353 study period. The glacier terminus retreated by 5811±20 m between 1947–2019 yielding

354   an annual retreat rates of −80.7 m yr⁻¹ (Figure 6b). Despite experiencing small readvances
355   or relatively stable positions during some years, this didn't compensate for the massive
356   overall retreat during this 72-year period. Stevenson Glacier retreated by 5541±20 m
357   during the more recent retreat period (1988-2019), corresponding to an annual retreat
358   rate of −178.7 m yr⁻¹ which is seven times higher than it was observed for Brown Glacier
359   during the same time (Figure 6b). The largest readvance was in 2005-2008 when glacier
360   terminus extended by 2118±20 m but this was followed by a larger retreat of −3846±20 m
361   yr⁻¹ between 2008-2009 (Figure 7).

362
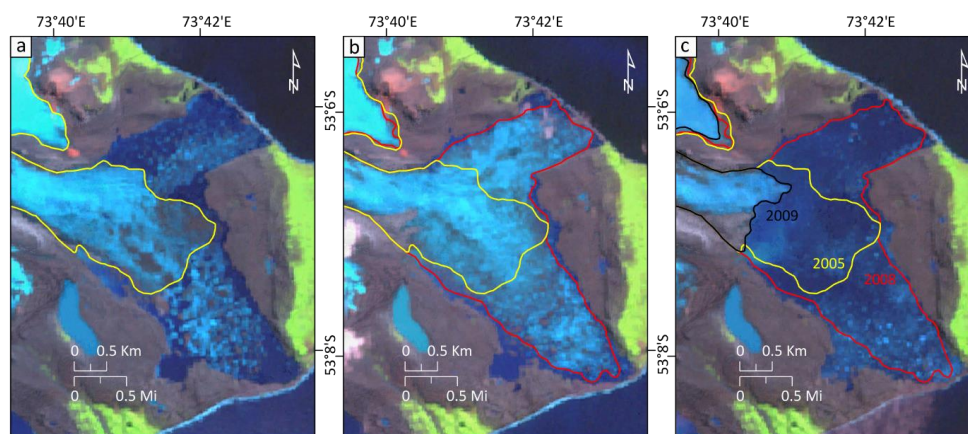
363

364   **Figure 7**. Stephenson Glacier advance and retreat in 2005–2008–2009. a – Landsat 7
365   ETM, 21/01/2005. b – Landsat 7 ETM, 04/02/2008. c – Landsat 7 ETM, 06/02/2009.

366

367   **5.3 Surface debris cover changes in 1988-2019**

368   We found that surface debris cover increased for all glaciers on Heard Island except
369   those facing northwest and for glaciers on the Laurens Peninsula. Overall debris cover
370   increased from 18.2±1.1 km² in 1988 to 29.0±1.6 km² in 2019. This increase in debris-
371   covered area occurred despite a large decrease in corresponding glacier area over this
372   period. The change equates to an increase in the proportion of debris-covered surface
373   area from 7.0±6.0 % in 1988 to 12.8±5.5 % in 2019 (Figure 8).

374   The mean upper limit (or maximum elevation) of the debris cover shifted from 285±20 to
375   605±20 m a.s.l. between 1988 and 2019 for all debris-covered glaciers on Heard Island.
376   The mean elevation of debris-covered parts also moved upwards from 165±20 to 410±20
377   m a.s.l. during this time. Southwest-facing Gotley Glacier had the highest mean upper
378   limit of surface debris cover with an elevation of 985±20 m a.s.l. Glaciers at Laurens
379   Peninsula had a small debris cover in 1988 but had become debris-free by 2019.

380

14
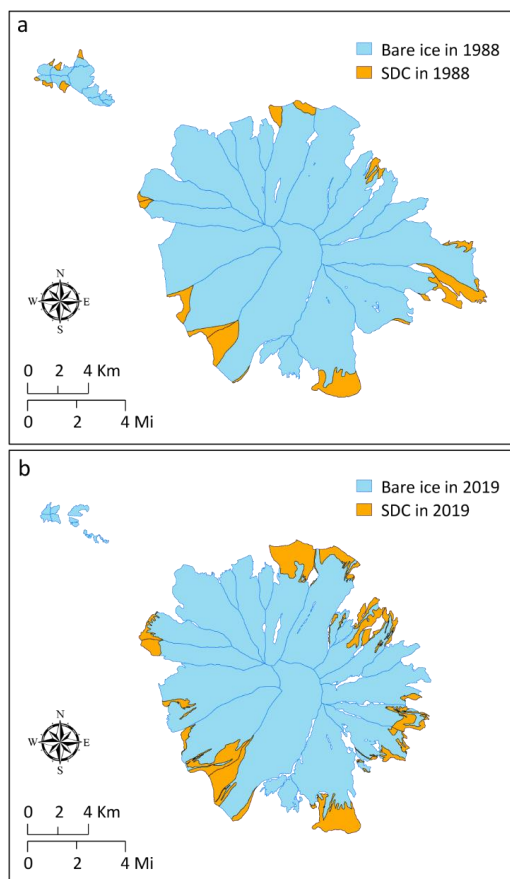
Figure 8. Decrease in bare ice and increase in surface debris cover (SDC) on Heard Island glaciers between 1988 (a) and 2019 (b).

6 Discussion

6.1 Glacier retreat and climate drivers

The relationship between climate and glacier changes in the Heard Island region must be considered cautiously because no local long-term weather station data are available. Instead, 2m surface air temperatures from ERA5 reanalysis (Soci et al., 2024) (0.5x0.5 deg) from a region encompassing Head Island (50-53° S, 70-73° E) were investigated between 1947 and 2019. Comparison between the first (1947–1959) and last (2009–2019) decades show summer temperature (NDJFM) increase by 0.7 °C which is consistent with previous record by Thost and Truffer (2008) who observed 0.8 °C increase of the summer temperatures between the 1948–1955 and 1997–2005 epochs. As shown in Figure 9a, a warming trend of the mean annual summer temperatures is also consistent with the increasing rate of glacier melting over the last 72 years. The period from 1980s onwards

15

397   is particularly notable for increasingly frequent and extreme positive temperature
398   anomalies relative to the long-term mean (Figure 9b).

399   Maritime glaciers such as those on Heard Island are particularly sensitive to air
400   temperature changes (e.g. Anderson and Mackintosh, 2006; Davies et al., 2014).
401   Warming causes the frequent precipitation to fall as rain rather than snow, decreasing
402   surface albedo over the glaciers and leading to increased absorption of short-wave
403   radiation and surface melt. Warmer temperatures also increase melt rates due to strong
404   turbulent exchange in these windy environments (e.g. Anderson et al., 2010; Anderson
405   and Mackintosh, 2012). For these reasons, the observed summer temperature increases
406   over the last 70 years are likely an important driver of ongoing glacier recession on Heard
407   Island. However, few precipitation measurements exist for Heard Island (Thost and
408   Truffer, 2008), and Favier et al. (2016) showed that retreat of the Cook Ice Cap on the
409   relatively nearby Kerguelen Islands is likely due to atmospheric drying since the 1960s
410   rather than atmospheric warming. Further observations and modelling are required to
411   provide more confidence in our interpretation that climate warming was largely
412   responsible for driving recent glacier retreat on Heard Island.

413   Our new glacier inventories indicate that Heard Island glaciers experienced overall
414   negative glacier mass balance between 1988 and 2019. This finding is supported by
415   satellite-based geodetic mass balance estimates for all Heard Island glaciers extracted
416   from the global study of Hugonnet et al. (2021) (Figure 10). However, a different mass
417   balance estimate derived from a mixed method that incorporates in situ observations
418   (Dussaillant et al., 2024) shows a positive geodetic mass balance trend between 1976
419   and 1998, in contrast to our observed glacier area reduction during the same period. This
420   mismatch (Figure 10) is likely due to the lack of direct mass balance observations to
421   constrain the estimates of Dussaillant et al. (2024) in this remote region.

422   The warming trend evident in ERA5 data in the Heard Island region (0.7°C) is relatively
423   small to the observed 1.1°C warming for the neighbouring Kerguelen Island between
424   1951-2020 (Nel et al., 2023) but it is in agreement with general Southern Ocean warming
425   trend since 1950s (Auger et al., 2021; Li et al., 2023). The primary driver of atmospheric
426   and ocean warming in this region is the human-induced shift towards the positive phase
427   of the Southern Annular Mode (Pohl et al., 2021), which has caused an intensification and
428   poleward shift of the Southern Hemisphere westerly winds (Perren et al., 2020). Further
429   accelerated decline in ice cover and warming air temperatures in the Heard Island region
430   mean that the glaciers may be rapidly approaching an irreversible tipping point in the sub-
431   Antarctic (Bakke et al. 2021), impacting landscape, geomorphic and ecosystem
432   processes.

433   Volcanic activity is another potential factor that could be contributing to the accelerated
434   glacier melting on Heard Island. Glacier retreat might also be a trigger for enhanced
435   volcanism at Heard Island due to decompression of the underlying magma chamber (e.g.
436   Barr et al., 2018). Eruptions could cause significant melting of the ice or deposition of

437 tephra, while increases in geothermal heat may lead to greater basal melting, thereby
438 influencing glacier movement (Allison and Keage, 1986; Fox et al., 2021). However, given
439 the lack of direct evidence in satellite images for unusual melt or tephra cover, the fact
440 that accelerated glacier melt occurred on all Heard Island glaciers and not just a subset,
441 and also on nearby Kerguelen Islands (Berthier et al., 2009; Deline et al., 2024), we
442 consider that any volcanic drivers of glacier retreat are less important than climatic ones.

443
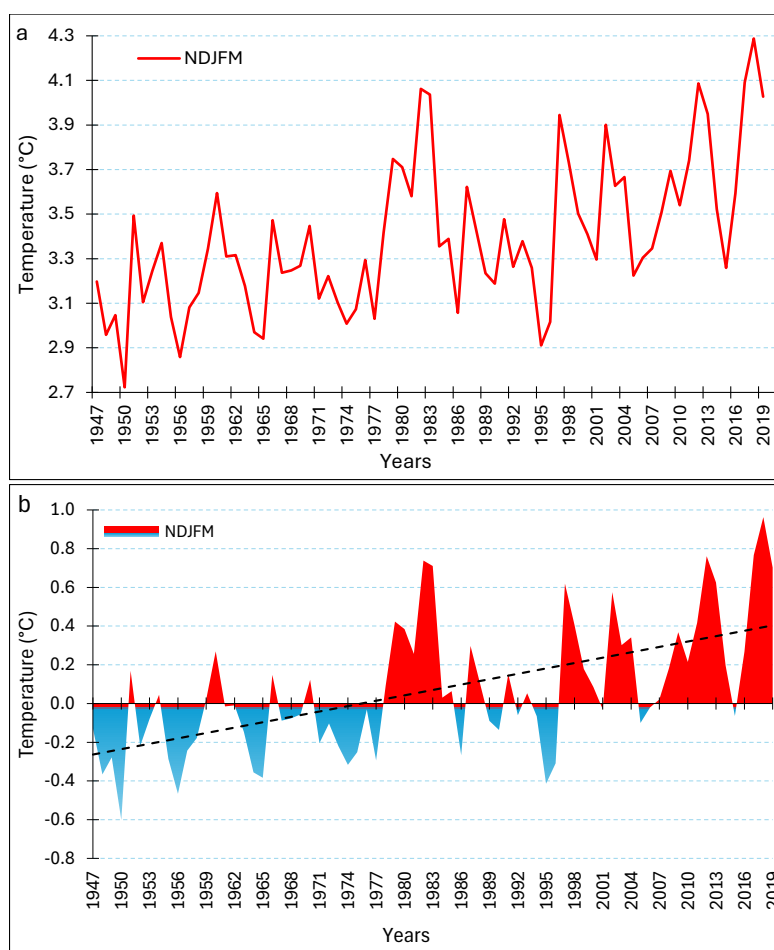
444

445

446 **Figure 9**. a - Mean annual warm season (NDJFM) temperatures (°C) for Heard Island
447 between 1947-2019. b - Time series of warm season (NDJFM) monthly air temperature
448 anomalies for the same period. The black dashed line on panel 'b' is the trend showing a
449 warming rate of 0.7°C over time. Both panels are based on the ERA5 2m surface air
450 temperature dataset.

451

452
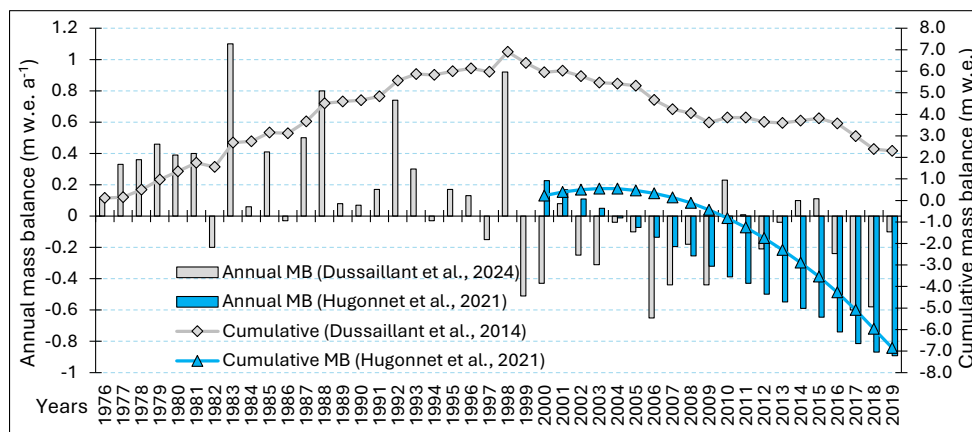
Figure 10. Mean annual geodetic mass balance (m w.e. a^{-1}) and cumulative mass balance (m w.e.) for all Heard Island glaciers between 2000-2019 (Hugonnet et al., 2021) and between 1976–2019 (Dussaillant et al., 2014).

6.2 The role of aspect and glacier lake formation on glacier retreat

We observed that higher rates of glacier retreat occurred on the eastern side of the island (Figure 3). Although climate data are sparce and a process-based modelling approach is required for further investigation, we expect this greater sensitivity of east-facing glaciers is due to factors such as increased foehn winds (and correspondingly warmer air temperatures) and reduced precipitation on the downwind side of the island. Our findings agree with previous studies of Heard Island glaciers (e.g. Thost and Truffer, 2008) and other studies in the sub-Antarctic region which show a similar asymmetry. For example, Berthier et al. (2009) observed that the eastern part of Cook Ice Cap on Kerguelen shrank 2.5 times more (~28%) than the western part (~11%) between 1963 and 2003. Similar observations have been made in South Georgia, where glacier decrease on the east coast was higher than on the windy and wet southwest coast during the second half of the 20th century (Gordon et al., 2008).

Comparison with other glacier retreat records from the southern mid to high latitudes (Figure 11) shows that lake formation is a key driver of accelerated glacier retreat. Brown Glacier on Heard Island initially experienced rapid retreat as a proglacial lake formed between 1947 and 1988; this is like Chamonix Glacier on Kerguelen which initially retreated in a lake but has been land terminating for several decades subsequently. The retreat rate of these glaciers once they become land-terminating is relatively linear and similar to the retreat rate of the land-terminating Fox and Franz Josef Glaciers in New Zealand (Purdie et al., 2020; Mackintosh et al., 2017) (Figure 11).

In contrast, Stephenson Glacier on Heard Island is notable for its unprecedentedly high terminus retreat, particularly between1988 and 2019 when the glacier retreated by

18

481 almost 5.5. km compared to 0.8 km at Brown Glacier (Figure 11). Lake formation at
482 Stephenson Glacier was much later than at Brown, and once a proglacial lake did form it
483 became extremely large. This is like the situation at Agassiz Glacier on Kerguelen which
484 retreated into its proglacial lake more recently than Chamonix Glacier (Deline et al.,
485 2024), and also Tasman Glacier in New Zealand which retreated more than 4.5 km in its
486 proglacial lake over recent decades (Mackintosh et al., 2017).

487
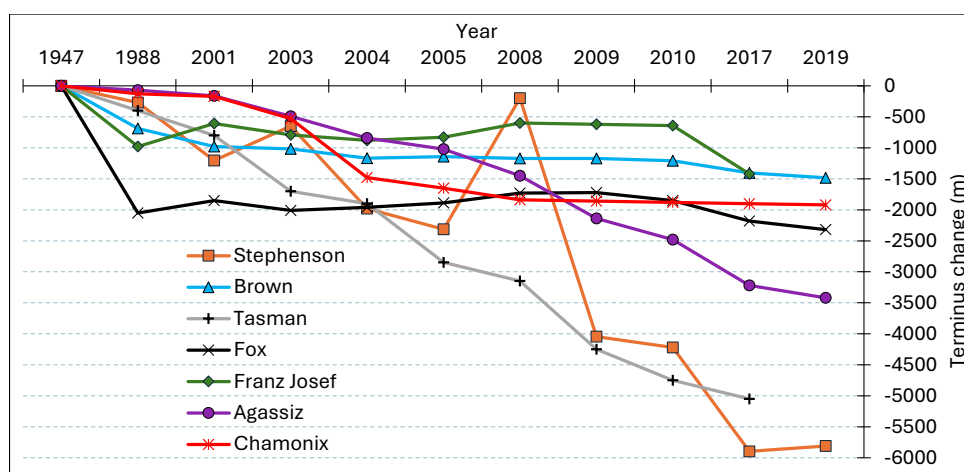
488

489 **Figure 11**. Cumulative terminus changes between 1947–2019 for Brown and Stephenson
490 glaciers (current study) compared to Agassiz and Chamonix glaciers on Kerguelen
491 (Deline et al., 2024) and Fox, Franz Josef and Tasman glaciers in New Zealand (Purdie et
492 al., 2020; Mackintosh et al., 2017).

493

494 The retreat of Stephenson Glacier warrants further discussion. In the 1950s, the glacier
495 had a long (~5.5 km) and low angle terminus compared to its counterparts and a
496 significant portion of that tongue was located near sea level (Figure 12). This is due to the
497 subtle and flatter topography of eastern Heard Island (see also Figure 1c). Low angle
498 glaciers are particularly sensitive to climate change (e.g. Oerlemans, 2001) and those
499 that terminate at sea level are subject to rapid surface and subaqueous ablation
500 throughout the year due to warm air temperatures and melting by seawater and
501 mechanical calving by tidal and wave action (Truffer and Motyka, 2016). Therefore, we
502 propose that, along with increased air temperatures, the high retreat rate of the
503 Stephenson Glacier may be related to the low topography and flat surface of the glacier
504 tongue and the negative impact of the very large lagoon connected to ocean water. We
505 also note that despite recent efforts to quantify ocean water properties in similar
506 environments (Mortensen et al., 2013; Straneo and Cenedese, 2015), rates of
507 subaqueous melting for Heard Island glaciers along with the water properties of the
508 associated lagoons are largely unknown and require further investigation. Finally, the

19

509 small readvances observed at Stephenson's Glacier are also characteristic of tidewater
510 glaciers which can undergo non-climatic advance and retreat cycles (Vieli, 2011).

511
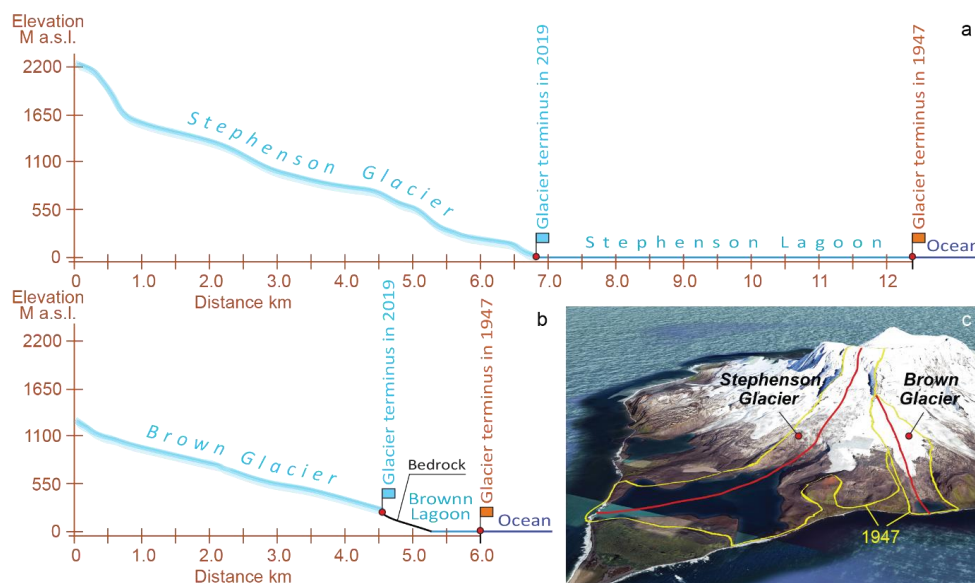
512

513 **Figure 12**. Longitudinal profiles based on Pléiades DSM, 2019. a – Stephenson Glacier; b
514 – Brown Glacier; c – Longitudinal profile paths (in red) for both glaciers on 3D view (©
515 Google Earth).

516

6.3 Impact of surface debris cover on glacier retreat

518 Despite an overall increase since 1988, surface debris has varied between individual
519 glaciers and some glaciers have contradicted the overall trend. e.g. A substantial amount
520 of surface debris cover was found on Stephenson Glacier in 1988 (~14%), mainly near the
521 terminus, which had almost disappeared by 2019 (~2.9%). This could be because the
522 glacier still had a low-angle tongue in 1988 that was favourable for debris accumulation
523 (e.g. Mölg et al., 2019), but that this debris-laden ice subsequently calved into the lake.
524 The debris cover at Stephenson Glacier prior to 1988 may have contributed to the
525 accelerated terminus retreat if debris was less than a few cm thick, as this would have
526 led to enhanced surface melting (e.g. Östrem, 1959). However, surface debris thickness
527 and properties have not been measured at Heard Island and this inference is speculative.

528 The most significant increase of surface debris cover was observed on northeast facing
529 Downes Glacier from ~9.8% in 1988 to ~31.6% in 2019, while the total area of this glacier
530 has only reduced by ~4.3% during the same period (Figure 3, 8). It is not clear what drove
531 this increase, though the lack of bare cliffs above the glacier (Figure 13) suggests a
532 subglacial source. More investigation is needed as there is no clear process that can

533 account for the observed development of surface debris cover at Downes Glacier relative
534 to other glaciers on Heard Island.

535

537 **Figure 13.** The most heavily debris-covered Downes Glacier within the Heard Island
538 (31/03/2024 © Google Earth).

539

540 A global assessment of surface debris cover by Scherler et al. (2018) uses RGIv6 outlines
541 for Heard Island delineated based on Spot images from 1988. We extracted these
542 outlines from Scherler et al. (2018) for our glacier sample from 1988 to compare results
543 (Figure 14). We found that Scherler et al. (2018) reported much higher percentage (25.2
544 %) of surface debris cover for Heard Island than our study (7.0) in 1988. This does not
545 even match within our uncertainty (±6.0 %). These differences are probably explained by
546 automatized method of global assessment of surface debris cover by Scherler et al.
547 (2018). Our approach uses accurate manual digitization, while automated mapping often
548 fails and manual corrections are required (e.g. Paul et al., 2013).

549
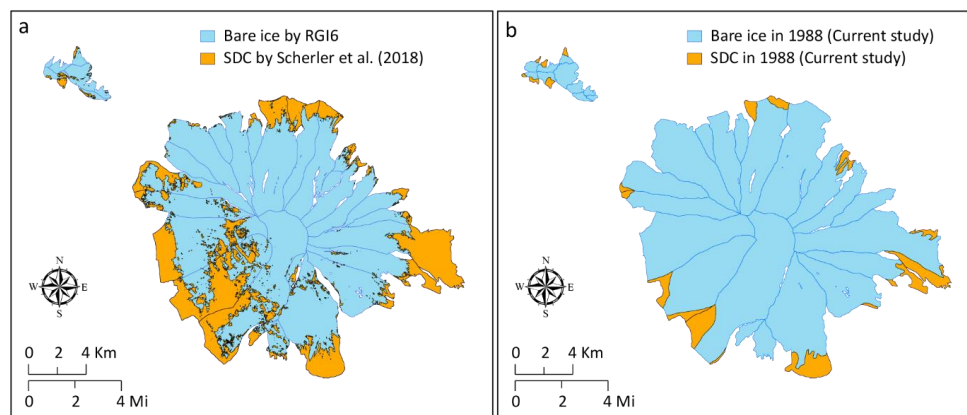
Figure 14. a – extracted surface debris cover (SDC) data from Scherler et al. (2018). Glacier outlines from RGIv6 from 1988; b – SDC from our study from 1988.

7 Conclusions

We present a multi-year glacier inventory based on historic topographical maps, medium-, and high-resolution satellite imagery and digital elevation/surface models. Our findings show that glaciers on Heard Island experienced significant area loss (22% or -0.31% yr^{-1}) over the 72-year period between 1947-2009, from 289.4 ± 6.1 km^2 to 225.7 ± 4.2 km^2 with an increasing rate of ice loss in recent decades. Our study also shows that the small and low elevation glaciers at Laurens Peninsula have experienced the highest recession rates of -1.1% yr^{-1} over the last 72 years.

We observed much higher glacier area decrease and terminus retreat on the east and southeast side of Heard Island. Although this asymmetry may have an underlying climate driver, for example due to increased foehn winds, topographic factors have clearly played a role; ice retreat on the eastern side of the island has been enhanced at low-elevation and low-angle tongues where glaciers have transitioned from land based to lake calving. Stephenson's Glacier is an exemplar of this behaviour. Surface debris cover has also increased on most Heard Island glaciers and could also be a contributor to accelerating ice loss.

Our new glacier inventory for Heard Island tracks changes in glacier extent, and dynamics, providing insights into the impact of climate change in this remote and sensitive region. Further work is required to test some of the ideas we have put forward in this paper regarding the different roles of climatic and non-climatic factors in driving ice retreat. The new inventory will also help to better understand how changes in glaciers affect biodiversity and ecosystems, which will inform conservation and management efforts at this World Heritage site.

22

Data availability

Will be submitted to GLIMS and can be used for future studies

Author contributions

LGT and ANM designed the conceptual framework for the study. LGT mapped glacier outlines and wrote the paper with input and feedback from ANM and WY.

Competing interests

The contact author has declared that neither they nor their co-authors have any competing interests.

Acknowledgements

Financial support

References

Allison, I. F.: A preliminary investigation of the physical characteristics of the Vahsel Glacier, Heard Island. ANARE Scientific Reports Series A(4); Glaciology. Publication 128. Canberra, Australian Government Publishing Service, 1980.

Allison, I. F., and Keage, P. L.: Recent changes in the glaciers of Heard Island. Polar Record. 23(144):255-272. doi:10.1017/S0032247400007099, 1986.

Allison, I., and Thost, D. E.: Heard Island glacier fluctuations and climatic change. Australian Antarctic Data Centre. data.aad.gov.au/metadata/records/ASAC_1158, 2000.

Anderson, B., Mackintosh, A., Stumm, D., George, L., Kerr, T., Winter-Billington, A., and Fitzsimons, S.: Climate sensitivity of a high-precipitation glacier in New Zealand. Journal of Glaciology, 56(195), 114-128. doi:10.3189/002214310791190929, 2010.

Anderson, B., and Mackintosh, A.: Temperature change is the major driver of late-glacial
and Holocene glacier fluctuations in New Zealand. Geology; 34 (2): 121–124. doi:
https://doi.org/10.1130/G22151.1, 2006.

Anderson, B., and A. Mackintosh.: Controls on mass balance sensitivity of maritime
glaciers in the Southern Alps, New Zealand: The role of debris cover, J. Geophys.
Res., 117, F01003, doi:10.1029/2011JF002064, 2012.

Aubert de la Rue, E.: "Un Voyage d'exploration dans les mers Australes. Iles Heard,
Archipel de Kerguelen, ile St. Paul."" Rev. de Geogr. Phys. et de Geol. Dynam. Univ.
de Paris, 11, 97-146, 1929.

Auger, M., Morrow, R., Kestenare, E. et al.: Southern Ocean in-situ temperature trends
over 25 years emerge from interannual variability. Nat Commun 12, 514.
https://doi.org/10.1038/s41467-020-20781-1, 2021.

Bakke, J., Paasche, Ø., Schaefer, J. M. and Timmermann, A.: Long-term demise of sub-
Antarctic glaciers modulated by the Southern Hemisphere westerlies. Scientific
Reports, 11, 10.1038/s41598-021-87317-5, 2021.

Barr, I. D., Lynch, C. M., Mullan, D., De Siena, L., and Spagnolo, M.: Volcanic impacts on
modern glaciers: A global synthesis. Earth-Science Reviews Vol., 182, 0012-8252,
https://doi.org/10.1016/j.earscirev.2018.04.008, 2018.

Berthier, E., Le Bris, R., Mabileau, L., Testut, L. and Rémy, F.: Ice wastage on the Kerguelen
Islands (49°S, 69°E) between 1963 and 2006. J. Geophys. Res. 114, F03005,
https://doi.org/10.1029/2008JF001192, 2009.

Berthier, E., Lebreton, J., Fontannaz, D., Hosford, S., Belart, J. M.-C., Brun, F., Andreassen,
L. M., Menounos, B., and Blondel, C.: The Pléiades Glacier Observatory: high-
resolution digital elevation models and ortho-imagery to monitor glacier change,
The Cryosphere, 18, 5551–5571, https://doi.org/10.5194/tc-18-5551-2024, 2024.

Bolch, T., Menounos, B., and Wheate, R.: Landsat-based inventory of glaciers in western
Canada, 1985–2005, Remote Sens. Environ., 114, 127–137,
https://doi.org/10.1016/j.rse.2009.08.015, 2010.

Bhambri, R., Bolch, T., Chaujar, R. K., Kulshreshtha, S. C.: Glacier changes in the Garhwal
Himalaya, India, from 1968 to 2006 based on remote sensing. Journal of Glaciology.
57(203):543-556. doi:10.3189/002214311796905604, 2011.

Budd, G. M.: Heard Island Expedition, 1963. Polar Record. 1964; 12(77):193-195.
doi:10.1017/S0032247400054619, 1964.

Budd, G. M.: Heard Island Reconnaissance, 1969. Polar Record. 1970;15(96):335-336.
doi:10.1017/S0032247400061131, 1970.

24

645 Budd, G. M. and Stephenson, P. J.: Recent glacier retreat on Heard Island. In Gow, A. J.
646   and others (editors). Proceedings of the International Symposium on Antarctic
647   Glaciological Exploration, Hanover NH, 1968: 449–58. IAHS Publication 86, 1970.

648 Budd, G. M.: Changes in Heard Island glaciers, king penguins and fur seals since 1947.
649   Papers and Proceedings of the Royal Society of Tasmania, vol. 133, no. 2, pp. 47-60,
650   https://doi.org/10.26749/rstpp.133.2.47, 2000.

651 Burgess, D. O., and Sharp, M. J.: Recent Changes in Areal Extent of the Devon Ice Cap,
652   Nunavut, Canada. Arctic, Antarctic, and Alpine Research, 36(2), 261–271.
653   https://doi.org/10.1657/1523-0430(2004)036[0261:RCIAEO]2.0.CO;2, 2004.

654 Cogley, J. G., Berthier, E., Donoghue, S.: Remote Sensing of Glaciers of the Subantarctic
655   Islands. In: Kargel, J., Leonard, G., Bishop, M., Kääb, A., Raup, B. (eds) Global Land
656   Ice Measurements from Space. Springer Praxis Books. Springer, Berlin, Heidelberg.
657   https://doi.org/10.1007/978-3-540-79818-7_32 , 2014.

658 Davies, B., Golledge, N., Glasser, N. et al.: Modelled glacier response to centennial
659   temperature and precipitation trends on the Antarctic Peninsula. Nature Clim
660   Change 4, 993–998. https://doi.org/10.1038/nclimate2369, 2014.

661 DeBeer, C. M., and Sharp, M, J.: Recent changes in glacier area and volume within the
662   southern Canadian Cordillera. Annals of Glaciology. 46:215-221.
663   doi:10.3189/172756407782871710, 2007.

664 Deline, P., Linge, H., Ravanel, L., et al.: Mapping of morainic complexes and
665   reconstruction of glacier dynamics north-east of Cook Ice Cap, Kerguelen
666   Archipelago (49°S). Antarctic Science. 36(2):75-100.
667   doi:10.1017/S0954102023000378, 2024.

668 Division of National Mapping.: Topographic map of Heard Island. Scale 1:50,000. MAP
669   G9182.H4. Produced by the Division of National Mapping, Dept. of National
670   Development. https://nla.gov.au/nla.obj-2545184819, 1964.

671 Drygalski, E. Von: "Geogr. von Heard Eiland.'? Deutsche Sudpolar Exped., 1901-3. Bd. 11,
672   Heft 3. Geog. u. Geol. 223-39, 1908.

673 Dussaillant, I., Hugonnet, R., Huss, M., Berthier, E., Bannwart, J., Paul, F., and Zemp, M.:
674   Annual mass changes for each glacier in the world from 1976 to 2023, Earth Syst.
675   Sci. Data Discuss. [preprint], https://doi.org/10.5194/essd-2024-323, in review,
676   2024.

677 Eis, J., van der Laan, L., Maussion, F., and Marzeion, B.: Reconstruction of Past Glacier
678   Changes with an Ice-Flow Glacier Model: Proof of Concept and Validation. Front.
679   Earth Sci. 9:595755. doi: 10.3389/feart.2021.595755, 2021.

680   Favier, V., Verfaillie, D., Berthier, E. et al.: Atmospheric drying as the main driver of
681   dramatic glacier wastage in the southern Indian Ocean. Sci Rep 6, 32396.
682   https://doi.org/10.1038/srep32396, 2016.

683   Fox, J. M., McPhie, J., Carey, R. J., Jourdan, F., and Miggins, D. P.: Construction of an
684   intraplate island volcano: The volcanic history of Heard Island. Bull Volcanol 83, 37.
685   https://doi.org/10.1007/s00445-021-01452-5, 2021.

686   Freudiger, D., Mennekes, D., Seibert, J., and Weiler, M.: Historical glacier outlines from
687   digitized topographic maps of the Swiss Alps, Earth Syst. Sci. Data, 10, 805–814,
688   https://doi.org/10.5194/essd-10-805-2018, 2018.

689   Gordon, J. E., V. M. Haynes, and A. Hubbard.: Recent glacier changes and climate trends
690   on   South   Georgia,   Global   Planet.   Change,   60(1–2),   72–84,
691   doi:10.1016/j.gloplacha.2006.07.037, 2008.

692   Granshaw, F. D. and Fountain, A. G.: Glacier change (1958–1998) in the North Cascades
693   National   Park   Complex,   Washington,   USA,   J.   Glaciol.,   52,   251–256,
694   https://doi.org/10.3189/172756506781828782, 2006.

695   Hall, D. K., Bayr, K. J., Schöner, W., Bindschadler, R. A., and Chien, J. Y. L.: Consideration
696   of the errors inherent in mapping historical glacier positions in Austria from the
697   ground   and   space   (1893–2001),   Remote.   Sens.   Environ.,   86,   566–577,
698   https://doi.org/10.1016/S0034-4257(03)00134-2), 2003.

699   HIMI (Heard Island and McDonald Islands) Marine Reserve Management Plan 2014-2024:
700   Dep. of the Env. Canberra 22, http://heardisland.antarctica.gov.au/, 2014.

701   HIMI   (Heard   Island   and   McDonald   Islands)   official   website.
702   https://www.antarctica.gov.au/antarctic-operations/stations/other-
703   locations/heard-island/climate-and-weather/ last access: August 2024.

704   Hock, R., Rasul, G., Adler, C., Cáceres, B., Gruber, S., Hirabayashi, Y., Jackson, M., Kääb,
705   A., Kang, S., Kutuzov, S., Milner, A., Molau, U., Morin, S., Orlove, B., and Steltzer, H.:
706   High Mountain Areas, in: IPCC Special Report on the Ocean and Cryosphere in a
707   Changing Climate, edited by: Pörtner, H. O., Roberts, D. C., Masson-Delmotte, V.,
708   Zhai, P., Tignor, M., Poloczanska, E., Mintenbeck, K., Alegría, A., Nicolai, M., Okem,
709   A., Petzold, J., Rama, B., and Weyer, N. M., 2019.

710   Hugonnet, R., McNabb, R., Berthier, E., Menounos, B., Nuth, C., Girod, L., Farinotti, D.,
711   Huss, M., Dussaillant, I., Brun, F., and Kääb, A.: Accelerated global glacier mass
712   loss   in   the   early   twenty-first   century,   Nature,   592,   726–731,
713   https://doi.org/10.1038/s41586-021-03436-z, 2021.

714   Kargel, J. S., Leonard, G. J., Bishop, M. P., Kääb, A., and Raup, B. (Eds.): Global Land Ice
715   Measurements   from   Space   (Springer-Praxis),   33   chapters,   876   pp.,
716   https://doi.org/10.1007/978-3-540-79818-7, 2014.

717   Kiernan, K., and McConnell, A.: Glacier retreat and melt-lake expansion at Stephenson
718   Glacier, Heard Island World Heritage Area. Polar Record. 38(207):297-308.
719   doi:10.1017/S0032247400017988, 2002.

720   Korneva, I. A., Toropov, P. A., Muraviev, A. Y., and Aleshina, M. A.: Climatic factors
721   affecting Kamchatka glacier recession. International Journal of Climatology, 1–25.
722   https://doi.org/10.1002/joc.8328, 2024.

723   Lambeth, A James.: "Heard Island. Geography and glaciology." Journal and proceedings
724   of the Royal Society of New South Wales 84(2), 92–98.
725   https://doi.org/10.5962/p.360589, 1951.

726   Lea, J. M., Mair, D. W. F., and Rea, B. R.: Evaluation of existing and new methods of tracking
727   glacier terminus change. Journal of Glaciology. 60(220):323-332.
728   doi:10.3189/2014JoG13J061, 2014.

729   Li, Z., England, M.H. and Groeskamp, S.: Recent acceleration in global ocean heat
730   accumulation by mode and intermediate waters. Nat Commun 14, 6888.
731   https://doi.org/10.1038/s41467-023-42468-z, 2023.

732   Mackintosh, A., Anderson, B., Lorrey, A., Renwick, J. A., Frei, P., and Dean, S. M.: Regional
733   cooling caused recent New Zealand glacier advances in a period of global warming.
734   Nat Commun 8, 14202. https://doi.org/10.1038/ncomms14202, 2017.

735   Maussion, F., Hock, R., Paul, F., Raup, B., Rastner, P., Zemp, M, Andreassen, L., Barr, I.,
736   Bolch, T., Kochtitzky, W., McNabb, R. and Tielidze, L: The Randolph Glacier
737   Inventory version 7.0 User guide v1.0, doi:10.5281/zenodo.8362857. Online
738   access: https://doi.org/10.5281/zenodo.8362857, 2023.

739   Mawson, D.: "The B.A.N.Z. Antarctic Research Expedition 1929-31." Geogr. Jour., 80, 105-
740   6, 1932.

741   Mortensen, J., J. Bendtsen, R. J. Motyka, K. Lennert, M. Truffer, M. Fahnestock, and S.
742   Rysgaard.: On the seasonal freshwater stratification in the proximity of fast-flowing
743   tidewater outlet glaciers in a sub-Arctic sill fjord, J. Geophys. Res. Oceans, 118,
744   1382–1395, doi:10.1002/jgrc.20134, 2013.

745   Mölg, N., Bolch, T., Walter, A., and Vieli, A.: Unravelling the evolution of Zmuttgletscher
746   and its debris cover since the end of the Little Ice Age, The Cryosphere, 13, 1889–
747   1909, https://doi.org/10.5194/tc-13-1889-2019, 2019.

748   Nagai, H., Fujita, K., Sakai, A., Nuimura, T., and Tadono, T.: Comparison of multiple glacier
749   inventories with a new inventory derived from high-resolution ALOS imagery in the
750   Bhutan Himalaya, The Cryosphere, 10, 65–85, https://doi.org/10.5194/tc-10-65-
751   2016, 2016.

752 Nel, W., Hedding, D. W., and Rudolph, E. M.: The sub-Antarctic islands are increasingly
753   warming in the 21st century. Antarctic Science. 35(2):124-126.
754   doi:10.1017/S0954102023000056, 2023.

755 Oerlemans, J.: Glaciers and Climate Change, 160 Pages, ISBN 9789026518133. 2001.

756 Östrem, G.: Ice Melting under a Thin Layer of Moraine, and the Existence of Ice Cores in
757   Moraine Ridges, Geogr. Ann., 41, 228–230,
758   https://doi.org/10.1080/20014422.1959.11907953, 1959.

759 Paul, F., Svoboda, F.: A new glacier inventory on southern Baffin Island, Canada, from
760   ASTER data: II. Data analysis, glacier change and applications. Annals of
761   Glaciology. 50(53):22-31. doi:10.3189/172756410790595921, 2009.

762 Paul, F., Barrand, N. E., Baumann, S. Berthier, E. Bolch, T. Casey, K. Frey, H. Joshi, S. P.,
763   Konovalov, V., Le Bris, R., Molg, N., Nosenko, G., Nuth, C., Pope, A., Racoviteanu,
764   A., Rastner, P., Raup, B., Scharrer, K., Steffen, S., and Winsvold, S.: On the accuracy
765   of glacier outlines derived from remote-sensing data, Ann. Glaciol., 54, 171–182,
766   https://doi.org/10.3189/2013AoG63A296, 2013.

767 Perren, B. B., Hodgson, D. A., Roberts, S. J., Sime, L., Van Nieuwenhuyze, W., et al.:
768   Southward migration of the Southern Hemisphere westerly winds corresponds with
769   warming climate over centennial timescales. Communications Earth and
770   Environment, 1, 10.1038/s43247-020-00059-6, 2020.

771 Pockley, P.: Climate change transforms island ecosystem. Nature 410, 616.
772   https://doi.org/10.1038/35070741, 2001.

773 Pohl, B., Saucède, T., Pergaud, J., Féral, J.-C., Richard, Y., Favier, V., et al.: Recent climate
774   variability around the Kerguelen Islands (Southern Ocean) seen through weather
775   regimes. Journal of Applied Meteorology and Climatology, 60, 10.1175/JAMC-D-20-
776   0255.1, 2021.

777 Purdie, H., Anderson, B., Chinn, T., Owens, I., Mackintosh, A., Lawson, W.: Franz Josef
778   and Fox Glaciers, New Zealand: historic length records. Glob. Planet. Change, 121,
779   41–52, https://doi.org/10.1016/j.gloplacha.2014.06.008, 2014.

780 Purdie, H., Bealing, P., Gomez, C., Anderson, B., and Marsh, O. J.: Morphological changes
781   to the terminus of a maritime glacier during advance and retreat phases: Fox
782   Glacier/Te Moeka o Tuawe, New Zealand. Geografiska Annaler: Series A, Physical
783   Geography, 103(2), 167–185. https://doi.org/10.1080/04353676.2020.1840179,
784   2020.

785 Radić, V., Bliss, A., Beedlow, A.C. et al.: Regional and global projections of twenty-first
786   century glacier mass changes in response to climate scenarios from global climate
787   models. Clim Dyn 42, 37–58, https://doi.org/10.1007/s00382-013-1719-7, 2014.

788   Raup, B. H., Khalsa, S. J. S., Armstrong, R. L., Sneed, W. A., Hamilton, G. S., Paul, F.,
789   Cawkwell, F., Beedle, M. J., Menounos, B. P., Wheate, R. D., Rott, H., Shiyin, L., Xin,
790   Li., Donghui, S., Guodong, C., Kargel, J. S., Larsen, C. F., Molnia, B. F., Kincaid, J. L.,
791   Klein, A., and Konovalov, V.: Quality in the GLIMS glacier database, in: Global Land
792   Ice Measurements from Space, edited by: Kargel, J. S., Leonard, G. J., Bishop, M. P.,
793   Kääb, A., and Raup, B. H., Springer Berlin Heidelberg, 163–182,
794   https://doi.org/10.1007/978-3-540-79818-7_7, 2014.

795   Scherler, D., Bookhagen, B., and Strecker, M. R.: Spatially variable response of Himalayan
796   glaciers to climate change affected by debris cover, Nat. Geosci., 4, 156–159,
797   https://doi.org/10.1038/NGEO1068, 2011.

798   Soci, C., Hersbach, H., Simmons, A., Poli, P., Bell, B., Berrisford, P., et al.: The ERA5 global
799   reanalysis from 1940 to 2022. Quarterly Journal of the Royal Meteorological Society,
800   150(764), 4014–4048. Available from: https://doi.org/10.1002/qj.4803, 2024.

801   Straneo, F., and C. Cenedese.: The dynamics of Greenland's glacial fjords and their role
802   in climate, Ann. Rev. Mar. Sci., 7, 89–112, doi:10.1146/annurev-marine-010213-
803   135133, 2015.

804   Stokes, C. R., Shahgedanova, M., Evans, I., and Popovnin, V. V.: Accelerated loss of alpine
805   glaciers in the Kodar Mountains, south-eastern Siberia, Glob. Planet. Change, 101,
806   82–96, https://doi.org/10.1016/j.gloplacha.2012.12.010, 2013.

807   Truffer, M., and R. J. Motyka.: Where glaciers meet water: Subaqueous melt and its
808   relevance to glaciers in various settings, Rev. Geophys., 54, 220– 239
809   doi:10.1002/2015RG000494, 2016.

810   Tachikawa, T., Hato, M., Kaku, M., and Iwasaki, A: Characteristics of ASTER GDEM version
811   2. In 2011 IEEE international geoscience and remote sensing symposium (pp. 3657-
812   3660). IEEE. https://doi.org/10.1109/IGARSS.2011.6050017, 2011.

813   Thost, D. E., and Truffer, M.: Glacier Recession on Heard Island, Southern Indian Ocean.
814   Arctic, Antarctic, and Alpine Research, 40(1), 199–214.
815   https://doi.org/10.1657/1523-0430(06-084)[THOST]2.0.CO;2, 2008.

816   Tielidze, L. G.: Glacier change over the last century, Caucasus Mountains, Georgia,
817   observed from old topographical maps, Landsat and ASTER satellite imagery, The
818   Cryosphere, 10, 713–725, https://doi.org/10.5194/tc-10-713-2016, 2016.

819   Tielidze, L. G. and Wheate, R. D.: The Greater Caucasus Glacier Inventory (Russia,
820   Georgia and Azerbaijan), The Cryosphere, 12, 81–94, https://doi.org/10.5194/tc-12-
821   81-2018, 2018.

822   Tielidze, L. G., Bolch, T., Wheate, R. D., Kutuzov, S. S., Lavrentiev, I. I., and Zemp, M.:
823   Supra-glacial debris cover changes in the Greater Caucasus from 1986 to 2014, The
824   Cryosphere, 14, 585–598, https://doi.org/10.5194/tc-14-585-2020, 2020.

825   Vieli, A.: Tidewater Glaciers. In: Singh, V.P., Singh, P., Haritashya, U.K. (eds) Encyclopedia
826   of Snow, Ice and Glaciers. Encyclopedia of Earth Sciences Series. Springer,
827   Dordrecht. https://doi.org/10.1007/978-90-481-2642-2_579, 2011.

828   Weber, P., Andreassen, L. M., Boston, C. M., Lovell, H., and Kvarteig, S.: An ~1899 glacier
829   inventory for Nordland, northern Norway, produced from historical maps. Journal
830   of Glaciology 1–19. https://doi.org/10.1017/jog.2020.3, 2020.

831   Zemp, M., M. Huss, E. Thibert, N. Eckert, R. McNabb, J. Huber, M. Barandun, H. Machguth,
832   S. U. Nussbaumer, I. Gartner-Roer, et al.: Global glacier mass changes and their
833   contributions to sea-level rise from 1961 to 2016. Nature 568 (7752):382–86.
834   doi:10.1038/s41586-019-1071-0, 2019.